# Design and Analysis of a Novel Variable Frequency Transformer

**Xianming Deng [1], Na Liu [1], Yuanda Sun [1], Qifen Guo [2], and Miaofei Zhang [3]**

[1] School of Electrical and Power Engineering
China University of Mining and Technology, Xuzhou, Jiangsu, 221116, China
xmdengcumt@126.com, liuna@cumt.edu.cn, 1026980211@qq.com

[2] State Grid Chuzhou Power Supply Company, Chuzhou, 239000, China
594507070@qq.com

[3] School of Computer Information Engineering, Chuzhou University, Chuzhou, Anhui, 239000, China
zhang_miaofei289@126.com

***Abstract*** ─ Cross-regional power supply and regional power grid interconnection is the future development of the power grid. At present, AC and DC asynchronous interconnection methods have disadvantages of complicated control and poor system stability. A grid interconnection solution based on variable frequency transformer (VFT) is a possible solution. Based on the introduction of the basic structure and operation principles of VFT, this paper presents a new structure in which a VFT and a drive motor share a core of electrical steel. The new structure VFT is modeled and analyzed by finite element analysis. Through the analysis of the air gap magnetic field of the VFT, the coupling analysis and operating characteristics analysis of the power winding and the control winding verify the design.

***Index Terms*** ─ Finite element analysis, grid interconnection, variable frequency transformer.

## I. INTRODUCTION

The interconnection of large power grids has been a development trend of power systems. The interconnection of power grids in various regions is also a necessary means of power grid development to a large scale. There are two main ways of interconnection of regional grids: AC synchronous and DC asynchronous. It is difficult for an AC synchronous interconnection to achieve large-scale long-distance transmission of electric energy; DC asynchronous interconnection relies on a large number of power electronic devices as the main converter equipment. Moreover, problems are complex, high installation and maintenance cost, and insufficient system stability. With long term study and innovation, the United States General Electric Company (GE) has proposed an interconnection device different from DC asynchronous and AC synchronous, this device uses a high-frequency wound induction motor as the core device of the VFT [1-2].

Since the first VFT was applied in 2004, wide attention has been paid, with related experiments and simulation carried out. When VFT is used in interconnection of local railway power grid and state power grid, it can meet the requirement of security and stability interconnection; When VFT is used for asynchronous interconnection of wind power grid and large power grid, the voltage stability and low voltage crossing ability of the wind farm can be improved. In the field of normal power transmission and new energy power generation, the way of using VFT interconnected power grids is a new direction for power systems and energy sources. VFT has a broad space for development.

In this paper, based on the structure of frequency conversion transformer, a novel structure of frequency conversion transformer is put forward, which integrates the driving motor by sharing the core of electrical steel. The finite element analysis [3] is carried out to demonstrate structural design by analyzing its advantages and characteristics compared with the original.

## II. THE VFT WORKING PRINCIPLE

As is shown in Fig. 1, the VFT is composed of a collector ring, a DC drive motor, and a rotating transformer [4]. The collector ring is used to conduct current between the resolver rotor winding and the three-phase stationary bus. When the stator side of the resolver is connected to the power grid, it will generate a rotating magnetic field at the same frequency in the transformer. If the rotor does not rotate, the rotating magnetic field will induce electromagnetic force (EMF) at the same frequency on the rotor side. Therefore the rotary transformer is equivalent to a conventional transformer. If the rotor rotates at a certain speed, the frequency of induced voltage on the rotor side is different from that on the stator side, so that the interconnection between

*Submitted On: March 15, 2018*
*Accepted On: June 17, 2018*

different frequency grids can be realized. If there is frequency differences between the two sides of the power grid, taking the frequency of the two power grid respectively as $f_1$, $f_2$, the rotor of the resolver transformer rotates continuously with the speed of the frequency deviation of the two power grids in proportion, the rotor speed at this time is:

$$n_r = \frac{60(f_1 - f_2)}{p}. \quad (1)$$

In Equation (1), $n_r$ and $p$ are respectively the mechanical speed and the number of pole pairs in the resolver rotor.

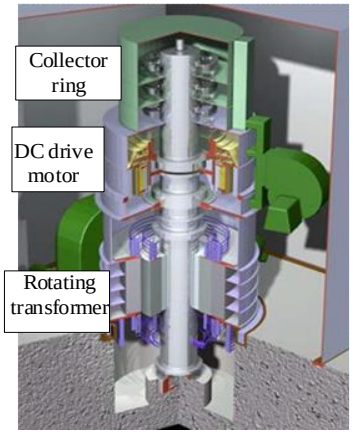


Fig. 1. VFT profile view.

The DC motor is coaxial with the rotor of the rotating transformer to control the rotating speed and power transfer of the rotor in the rotating transformer. In the case of interconnection between two power grids, the position of the resolver rotor related to its stator can be changed by adjusting the torque to drive the DC motor, so that the direction and the size of the power transmission can be changed [5]. The VFT is essentially a phase-shifting transformer with an adjustable phase angle. The expression of transmission power is as follows [6]:

$$P_{VFT} = \frac{V_1 V_2}{X_{12}} \sin(\theta_1 - \theta_2 - \theta_{rm}) = \frac{V_1 V_2}{X_{12}} \sin(\theta_{net}). \quad (2)$$

In Equation (2), $V_1$ is the VFT stator terminal three-phase voltage; $V_2$ is the three-phase synthesis voltage of VFT rotor side; $X_{12}$ is the reactance between the stator and rotor winding; $\theta_1$ is the angle of $V_1$; $\theta_2$ is the angle of $V_2$; $\theta_{rm}$ is the angle between the rotor and the stator. The relationship between the phase angle of the fixed rotor voltage phase and the principle of power transmission can be expressed in the phase diagram of Fig. 2.

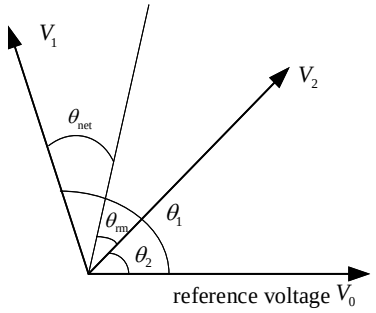


Fig. 2. Voltage phase of the VFT stator and rotor terminal.

## III. VFT DESIGN

### A. The basic structure of the proposed VFT

The original structure of the VFT system requires motor drive combination and the rotary transformer be connected in a coaxial way. The system structure is complicated, with a long axial shaft. Also, the number of bearing seats is large, and the amplitude of the shaft vibration and the waveform is high as well. In this paper, on the basis of the original structure in Fig. 1, a new structure of VFT is proposed. The rotating transformer and the driving motor share a set of stator and rotor core, which combine the rotating transformer and the driving motor. The method can reduce the axial length of the frequency transformer, simplify its structure, reducing the size of the frequency transformer and saving the manufacturing cost. It can also facilitate the assembly and maintenance on site, thus improving the operation reliability to a certain extent.

As the proposed transformers and drive motors share a set of stator and rotor core, the coupling effect should be taken. To facilitate design, the driving motor is equipped with a permanent magnet synchronous motor (PMSM). The number of stator slot in the PMSM is 48, the rotor structure is built-in and the pole logarithm is 6. On this basis, by increasing the stator slot of the PMSM, a set of stator control winding is added. 24 rotor slots with armature windings are used, which combine the drive motor and the rotating transformer. The longitudinal section, B-B section and circuit diagram of the structure are shown in Fig. 3, Fig. 4, and Fig. 5, respectively.

The numbers in Fig. 3 to Fig. 5 represent: 1-Stator core; 2-Stator slot; 3-Three-phase power winding of the stator; 4-Three-phase control winding of the stator; 5-Rotor core; 6-Rotor slot; 7-Permanent magnet slot; 8-Three-phase power winding of the rotor; 9-Permanent magnets; 10-Three-phase slip ring; 11-Three-phase brush; 12-Shaft. GRID1 represents three-phase grid 1, and GRID2 represents three-phase grid 2; RPC is a reversible inverter. The yellow part in Fig. 4 is the power winding of the stator rotor, the blue part is the control winding of the stator, and the green part is the permanent magnet of

the rotor. The three-phase power winding of the stator in Fig. 5 is connected to the GRID1, and the control winding of the stator is connected to a reversible inverter. On the rotor side, the power windings of the rotor in the rotor slots are connected to the GRID2 via three-phase slip rings and three-phase brushes on the shaft.

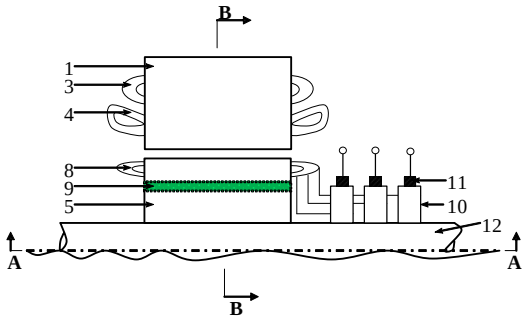


Fig. 3. Longitudinal profile diagram of the VFT.

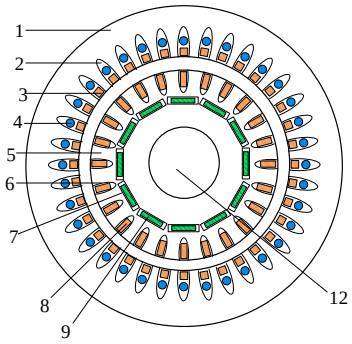


Fig. 4. B-B sectional view of the VFT.

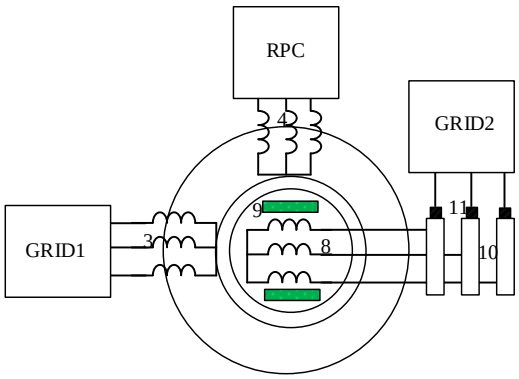


Fig. 5. Circuit structure diagram of the VFT.

### B. The working principle of the new structure of the VFT

The VFT consists of two subsystems: the variable voltage variable frequency (VVVF) subsystem and the permanent magnet synchronous drive subsystem. The VVVF subsystem consists of a stator core, a rotor core, a set of three-phase power winding of the stator, a set of three-phase power winding of the rotor, three-phase slip rings and brushes. The number of pole pairs in the three-phase power windings in the stator equals to that in the rotor windings, which is set to $P_p$; The power windings of the stator are directly connected to the GRID1, and the power windings of the rotor are connected to GRID2 via slip rings and brushes. The permanent magnet synchronous drive subsystem is composed of the stator core, the rotor core, the three-phase control winding of the stator and the permanent magnet. The number of pole pairs in the stator control windings is the same as that in the permanent magnet, which is set to be $P_c$. The stator control winding is connected and controlled by a reversible inverter. Based on the knowledge of motor, it is possible to transfer the AC power between the power windings of the stator and the rotor, satisfying the following formula:

$$U_1 = \frac{N_1 f_1 k_{w1}}{N_2 f_2 k_{w2}} \cdot U_2 . \tag{3}$$

In the formula, $U_1$ and $U_2$ are the voltage of the power winding in the stator and rotor respectively; $N_1$ and $N_2$ are the turns of power windings in stator and rotor respectively, and their winding coefficients are respectively $k_{w1}$, $k_{w2}$. The frequency of the power winding in the stator and rotor is recorded as $f_1$, $f_2$. It is known from the formula (3) that the voltage is changed by designing or adjusting the number of turns of the power winding in the stator and rotor.

When the frequency of the power grid connected to the stator and the rotor is unequal, it is known from the previous analysis that the rotational speed *n* of the rotor in the stable operation should satisfy the following formula:

$$n_r = \frac{60(f_1 - f_2)}{p_p} . \tag{4}$$

The VVVF subsystem and the permanent magnet synchronous drive subsystem share the same rotor, so the speed of the PMSM in the drive subsystem must also meet formula (4). The PMSM can be controlled by the reversible inverters and meet the speed requirement. By controlling the inverters, we can control the torque exerted on the rotor of PMSM, thus controlling the power transmission angle $\theta_{net}$ to achieve the purpose of controlling the size and direction of transmission power on both sides.

## IV. FINITE ELEMENT ANALYSIS OF THE PROPOSED VFT

Specific parameters of the proposed VFT are shown in Table 1. In this paper, the finite element method is used for structural modeling.

Table: 1 Design parameters of the proposed VFT

| Parameter | Numerical Value |
|---|---|
| Rated power/MW | 100 |
| Phase | 3 |
| PMSM control winding phase | 3 |
| Rated voltage of two sides power grid/kV | 15 |
| Frequency range of interconnected power grid/Hz | 45-55 |
| Control circuit rated voltage/kV | 1 |
| Drive circuit rated power/kW | 30 |
| Power winding pole pairs | 1 |
| Pole-arc factor | 0.72 |
| Stator outer diameter/mm | 11200 |
| Stator inner diameter/mm | 6740 |
| Rotor outer diameter/mm | 6710 |
| Rotor inner diameter/mm | 1250 |
| Rated speed/(r/min) | 300 |
| Rated frequency difference/Hz | ±5 |
| Rated efficiency of VFT/% | 92 |

**A. Analysis of air gap magnetic field**

When the power windings of the stator are excited, circuit of the rotor winding is set to the open state, with three-phase windings a supply of 15kV, 50Hz three-phase symmetrical rated voltage. The distribution of the flux lines of the VFT, the air-gap flux density and the air-gap flux density harmonics are shown in Fig. 6 (a), Fig. 6 (b) and Fig. 6 (c). As can be seen from Fig. 6 (a), when the circuit of the stator windings is excited, the internal magnetic field turns into one pole pair and the magnetic line distribution is proper. From Fig. 6 (b) and Fig. 6 (c), it can be seen that the air gap flux density is basically sinusoidal in one cycle with less odd harmonic content when the circuit of stator power winding gets excitation. Because the winding is three phase symmetry, there is no even subharmonic in the air gap magnetic density.

When permanent magnets are excited, the circuit of the power windings in the stator and the rotor, as well as the circuit of the control windings in the stator are opened. The rotor speed is 300r/min, and the permanent magnet excitation direction is radial, the distribution of the flux lines of the VFT, the air-gap flux density and the air-gap flux density harmonics are shown in Fig. 7 (a), Fig. 7 (b) and Fig. 7(c). As can be seen from Fig. 7 (a), when the permanent magnets are excited, their internal magnetic fields are distributed into six pole pairs. Some magnetic saturation occurs at the magnetic bridge, which limits the magnetic flux leakage, but there is also some weak magnetic flux leakage. The magnetic circuit design is reasonable. As can be seen from Fig. 7 (b) and Fig. 7 (c), when the permanent magnets are excited alone, the air gap flux density has a six-period sinusoidal distribution in the air-gap circumference. Because the width of the six permanent magnets the rotor is limited, the sine degree in each cycle is deficient, and the harmonic content is relatively large.

When the power windings of the stator and permanent magnet get the excitation at the same time, we set the rotor power winding and the stator control winding to the open state. In this case, the distribution of the flux lines in the VFT, the air-gap flux density and the number of air-gap flux density harmonics are shown in Fig. 8 (a), Fig. 8 (b) and Fig. 8 (c). As can be seen from Fig. 8 (a), generally, the internal magnetic field has one pole pair, and the pole pair consists of six smaller poles. In the edge of the polar magnetic fields, the interference of the six smaller pairs is obvious. In general, the distribution of the internal magnetic field is reasonable when getting excited together. As can be seen from Fig. 8 (b), when the stator power windings and the permanent magnets are excited together, the air gap magnetic density is superposed by one pair pole as a basic excitation plus six smaller pair poles, and a sinusoidal distribution is generated on the whole air gap circumference. In part, it becomes a sine distribution of six cycles. From the harmonic orders of Fig. 8 (c), it can be seen that period one and six have the most of the harmonic content meanwhile the clutter is relatively less.

The analysis of the three cases is taken when $t$=50ms.

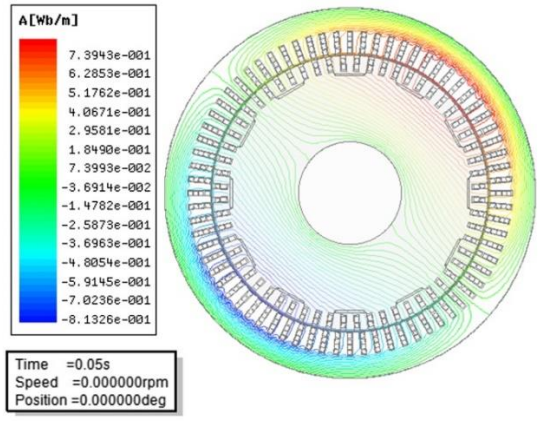


(a) Distribution magnetic force lines

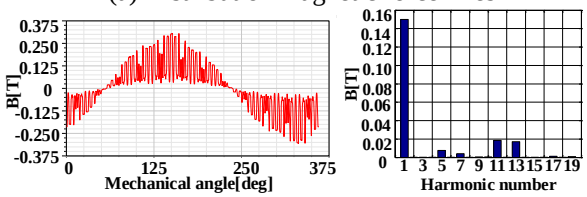


(b) Air gap magnetic flux density (c) Harmonic orders

Fig. 6. Independent excitation on stator power winding.

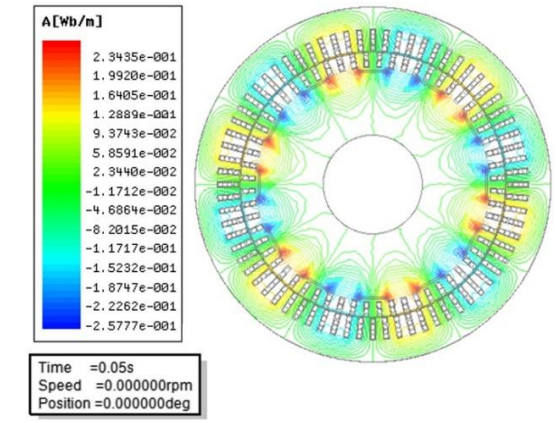


(a) Distribution curve of magnetic force line

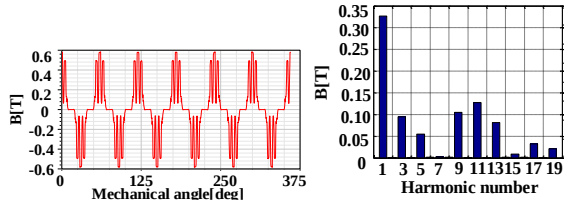


(b) Air gap magnetic flux density (c) Harmonic orders

Fig. 7. Independent excitation on permanent magnets.

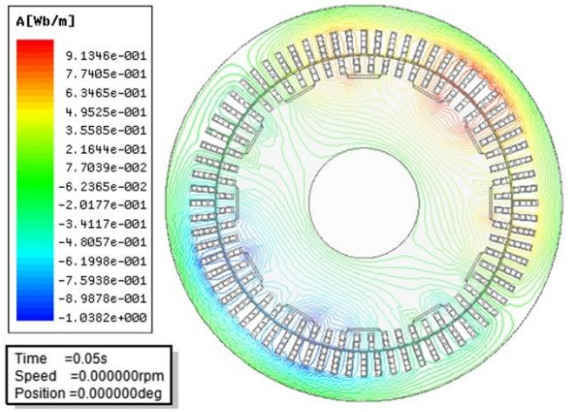


(a) Distribution curve of magnetic force line

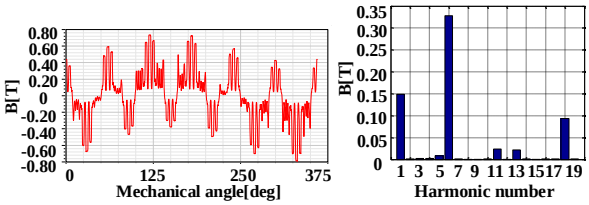


(b) Air gap magnetic flux density (c) Harmonic orders

Fig. 8. Excitation on stator power windings and permanent magnets.

**B. Coupling analysis of the power windings and the control windings**

Because the rotating transformer and the driving motor share the same iron core, their coupling relationship must be considered. When the pole pairs number of three phase power windings and the number of pole pairs in control windings meet the following conditions $P_c >> P_p$, $P_c = 2 \times k \times P_p$, ($k$=1, 2, 3……), the direct coupling relationship between three-phase power windings and three-phase control windings will be eliminated, and the loss power of the power and control windings will be greatly reduced. Therefore, structural design of the VVVF subsystem and permanent magnet synchronous drive subsystem pole pairs is particularly important. In this paper, the VVVF subsystem power winding pole pairs $P_p = 1$, the permanent magnet synchronous control subsystem pole pairs $P_c = 6$. By analysing the induced electromotive force, we can get to know the mutual influence due to coupling between the power control windings.

***(1) The influence on rotor winding excited by stator control winding***

When the circuit of the state power winding is not connected to the power grid, the control winding of the stator is applied with a rated voltage of 50 Hz and 1 kV which is shown in Fig. 9 (a) from t=100ms, and the induced EMF generated in the power winding of the rotor is shown in Fig. 9 (b). The amplitude of the induced voltage is 2.2V, which is about 0.15% of the rated voltage on the rotor side power winding. It can be seen that when the stator is excited, there is almost no potential induction in the power winding.

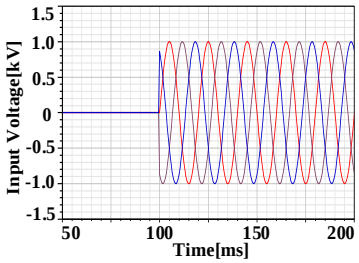


(a) Voltage on stator control winding

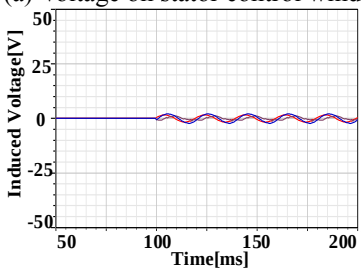


(b) Induction voltage on rotor power winding

Fig. 9. Influence of stator windings on rotor power windings.

***(2) The influence on stator control winding excited by stator and rotor power windings***

The circuit of control winding on stator is open

from the moment $t$=100ms, which is shown in Fig. 10 (a). Apply the same excitation 15kV, 50Hz voltage to the stator and rotor power windings, and the rotor does not turn at this time. The induction EMF of the control windings in the stator, as is shown in Fig. 10 (b), is about 0.6V, about 0.6% of the rated stator voltage value. It can be seen that when the power winding is excited, there is little induction EMF in the control winding.

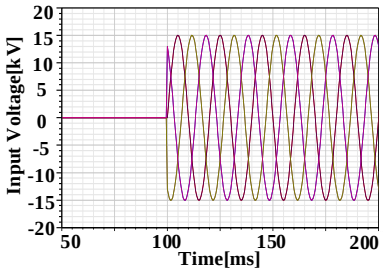


(a) Voltage on stator power winding

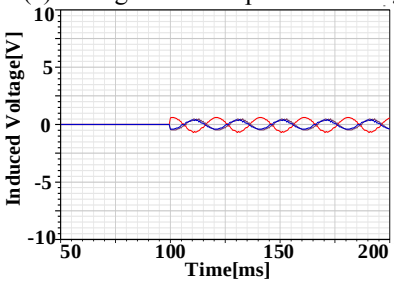


(b) Induction voltage on stator control winding

Fig. 10. The control winding EMF inducted by the stator and rotor power windings.

The simulation results show the weak coupling relationship between the power winding and the control winding of the VFT which realizes the decoupling of the two windings and meets the design requirements.

### C. Analysis of operation characteristics

#### *(1) No-load operation state*

The power winding of the stator is connected to the 15kV and 50Hz power grid, the rotor speed is zero, the control winding of the stator has no control voltage, and the circuit of the power winding in the rotor is open. At $t$=800ms, the power frequency of the stator power winding changes to 45 Hz, the voltage amplitude is constant, and the rotor speed rotates reversely at 300 r/min at this time. According to the working principle of the VFT, it is known that the frequency of the induction voltage in the rotor power windings should remain unchanged at 50Hz. Figure 11 (a) is the stator winding voltage curve, Fig. 11 (b) is the speed curve of the rotor. Figure 11 (c) is the induced EMF waveform of the rotor power winding. It can be seen that when the frequency of the stator side power supply changes, the induced EMF of the rotor keeps constant at 50 Hz, and the waveform is ideal. Figure 11 (d) shows the stator power winding current waveform. Under no-load condition, the peak value of the current is about 50A. After a period of speed change, the dynamic steady state is reached. When smoothing, the peak value is about 57A. Figures 11 (e) and (f) show the curves of iron loss and copper loss, respectively. It can be seen that the iron loss is 81.54kW before the frequency of the stator power winding changes, and the iron loss is about doubled after the changes. This is due to the constant of the stator voltage, the decrease of frequency and the increase of magnetic induction intensity. The factors above result in the increase of iron consumption. The copper consumption is also increased from 36.9kW to 49.8kW, due to the increase of current.

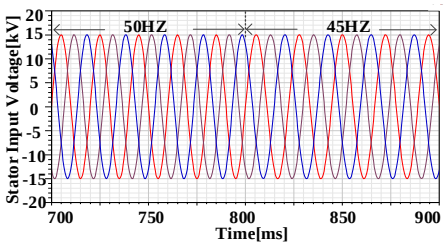


(a) Voltage on stator winding

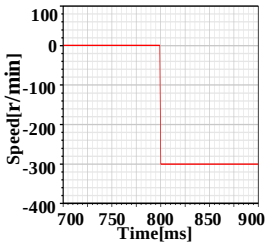


(b) Rotor speed

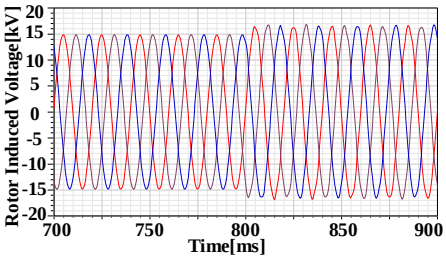


(c) Induction voltage on rotor winding

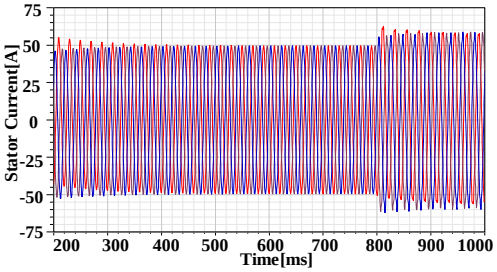


(d) Current on stator winding

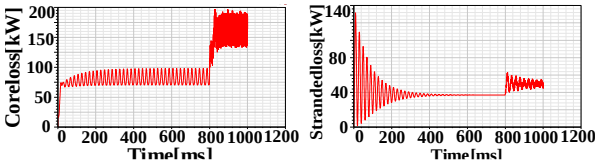


(e) Iron loss (f) stator copper loss

Fig. 11. Analysis of rotor side on no-load open state.

***(2) Load running state***

When the circuit of the rotor winding is connected to the resistance, it can simulate the load situation of the rotor side. The stator power windings are connected to the 15kV and 50Hz power grid. The rotor speed is zero and the stator control windings have no control voltage. At this point, the rotor side correspondingly induces an EMF at the same frequency 50 Hz.

At $t$=800ms, the grid frequency of the stator-side is changed to 45Hz, the voltage is constant. At this time the rotor speed rotates reversely at 300 r/min. Figure 12 (a) is the voltage variation curve of the stator side, and Fig. 12 (b) is the speed change curve of the rotor. Figure 12 (c) is induction voltage waves of the rotor side. The frequency of the rotor side voltage remains the same whenever the stator voltage frequency changes, which realizes the grid connection of two different frequencies. Figures 12 (d) and (e) are current waveforms of the stator and rotor side, with amplitudes about 510A and 508A respectively. After a change of speed, they will enter a steady state and eventually become stable. Figures 12 (f) and (g) are the curves of iron consumption and power transfer respectively. It is known that the iron consumption is about 37.06kW before the stator side frequency and the speed changes. The iron consumption changes to 92.8kW after the change. For the power transferred on the stator side, it can be seen from Fig. 12 (g) that before the stator side frequency changes at $t$=800ms, the transmission power is 3.68MW, and after the change the transmission power is 4.21MW.

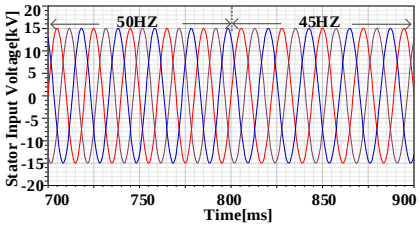


(a) Voltage on stator winding

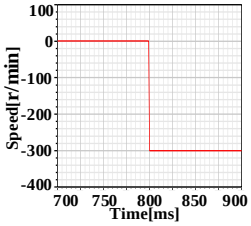


(b) Rotor speed

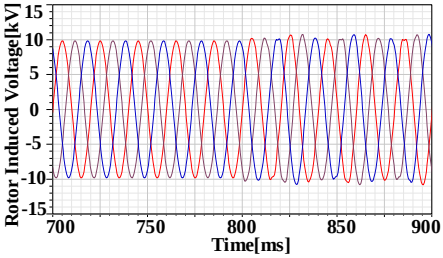


(c) Induction voltage on rotor winding

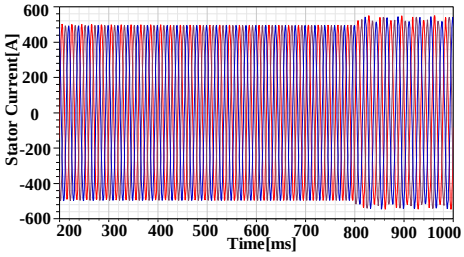


(d) Current on stator winding

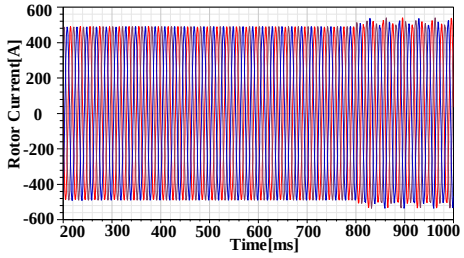


(e) Current on rotor winding

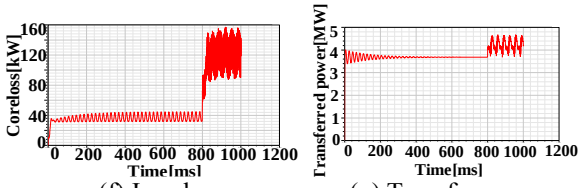


(f) Iron loss (g) Transfer power

Fig. 12. Analysis of the rotor side on the load state.

The proposed VFT can change the driving torque of the permanent magnet synchronous drive subsystem by adjusting the stator control windings. In this way, we can control the size and direction of the active power delivered by the VFT. Change the amplitude and power angle of the stator winding voltage when the rotor side is on load state, that is, at first, the stator side is connected to the 15kV, 45Hz power grid, and the rotor rotates in the reverse direction of 300r/min, then change the amplitude and power angle of the stator winding voltage at $t$=800ms, and the result of power transfer is shown in Fig. 13.

In Fig. 13 (a), when $t$=800ms, the control voltage is positive phase sequence 750V, 30Hz, power angle is 10°, the input power of permanent magnet synchronous system is about 0.628MW, the transmission power is 7.57MW. In Fig. 13 (b), the control voltage is positive phase sequence 1000V, 30Hz, power angle is 15°, the input power of permanent magnet synchronous system

is about 0.9425MW, and the transmission power is 10.82MW. Both cases basically meet the power transfer relationship, to a certain extent, proving that the proposed VFT design is reasonable.

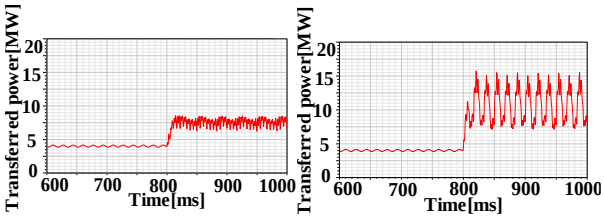


Fig. 13. Transfer power at different control voltage.

## V. CONCLUSION

In this paper, a structure of inverter with integrated drive motor is proposed. This VFT is modeled and analyzed by finite element analysis. By comparing and analyzing the magnetic field relationship between the VFT subsystem and the permanent magnet synchronous control system under their respective operation and interaction, the analysis of the air gap magnetic field, the coupling analysis of the power winding and the control winding shows that their mutual influence is small, and thus a reasonable decoupling is realized. The simulation of grid connection between stator and rotor power winding is carried out. After frequency mutation at one side, adjusting the rotor speed by controlling winding can keep the frequency of the other side relatively stable, and transmit power smoothly. By changing the input torque and power provided by the permanent magnet control system, the power of the winding will change along the rotor side, which proves effectiveness of the proposed VFT structure.

## ACKNOWLEDGMENT

This work has been supported by the Top-notch Academic Programs Project of Jiangsu Higher Education Institutions PPZY2015B132 and the National Natural Science Foundation of China (U1610113).

## REFERENCES

[1] B. B. Ambati and V. Khadkikar, "Variable frequency transformer configuration for decoupled active-reactive powers transfer control," *IEEE Transactions on Energy Conversion*, vol. 31, no. 3, pp. 906-914, 2016.

[2] A. Merkhouf, S. Upadhyay, and P. Doyon, "Variable frequency transformer - An overview," *Power Engineering Society General Meeting, IEEE*, 2006.

[3] R. Lerch, M. Kaltenbacher, H. Landes, J. Hoffelner, M. Rausch, and M. Schinnerl, "Advanced transducer modeling using the finite element method," *International Journal of Applied Electromagnetics & Mechanics*, vol. 17, no. 1, pp. 59-73, 2003.

[4] A. Merkhouf, P. Doyon, and S. Upadhuay, "Variable frequency transformer-concept and electromagnetic design evaluation," *IEEE Journals & Magazines*, vol. 23, no. 4, pp. 989-996, 2008.

[5] F. I. Bakhsh, M. Irshad, and M. S. J. Asghar, "Modeling and simulation of variable frequency transformer for power transfer in-between power system networks," *India International Conference on Power Electronics*, pp. 1-7, 2011.

[6] E. T. Raslan, A. S. Abdel-Khalik, M. A. Abdulla, and M. Z. Mustafa, "Performance of VFT when connecting two power grids operating under different frequencies," *IET International Conference*, pp. 1-6, 2010.

[7] K. Jemaï, "Intelligent integration strategies of wind farms in a super grid," *Journal of Intelligent & Fuzzy Systems*, vol. 31, no. 1, pp. 275-290, 2016.

**Xianming Deng** was born in Sichuan, China. He received his B.S., M.S., and Ph.D. in Electrical Engineering from China University of Mining and Technology, Jiangsu, China. He is currently a Professor in the School of Electrical and Power Engineering of China University of Mining and Technology. His current research interests include power electronics and motor drive.

**Na Liu** was born in Anhui, China. She received her B.S. in Electrical Engineering from China University of Mining and Technology, Jiangsu, China. She is currently receiving a Master education at China University of Mining and Technology. Her current research interests include power electronics and motor drive.

**Yuanda Sun** was born in Henan, China. He received his B.S. in Electrical Engineering from University of Electronic Science and Technology of China, Sichuan, China. He is currently receiving a Master education at China University of Mining and Technology. His current research interests include power electronics and motor drive.

**Qifeng Guo** was born in Jiangsu, China. He received his B.S. and M.S. in Electrical Engineering from China University of Mining and Technology, Jiangsu, China. He is currently an Electrical Engineer in State Grid Chuzhou Electric Power Supply Company. His current research interests include design and applications of permanent-magnet machines and drives, and distributed resources connected to power grid.

**Miaofei Zhang** was born in Inner Mongolia, China. She received her B.S. in Electronic Science and Technology and her M.S. in Communication and Information System from China University of Mining and Technology, Jiangsu, China. She is currently an Assistant in School of Computer Information Engineering of Chuzhou University. Her current research interests include wireless technology and micro-electromechanical systems.